A Journal of the Gesellschaft Deutscher Chemiker

Angewandte

GDCh

International Edition

Chemie

www.angewandte.org

Accepted Article

Title: Developing an Efficient Biosensor for In Vivo Quantification of Cu + and pH in the Brain Based on Rational Design and Synthesis of Recognition Molecules

Authors: Wei Liu, Hui Dong, Limin Zhang, and Yang Tian

To be cited as: *Angew. Chem. Int. Ed.* 10.1002/anie.201710863
Angew. Chem. 10.1002/ange.201710863

Link to VoR: http://dx.doi.org/10.1002/anie.201710863
http://dx.doi.org/10.1002/ange.201710863

WILEY-VCH

10.1002/anie.201710863

WILEY-VCH

COMMUNICATION

Developing an Efficient Biosensor for In Vivo Quantification of Cu^+ ions and pH Value in the Brain: Rational Design and Synthesis of Recognition Molecules

Wei Liu,[†] Hui Dong,[†] Limin Zhang, Yang Tian**

Abstract: An efficient biosensor was created for ratiometric monitoring of Cu^+ ions and pH in the brain using both current and potential outputs. A series of N, N-bis(2-(2-(ethylthio)ethyl)-based (NS4s) derivatives was designed for specific recognition of Cu^+ ions. After systematically evaluating the electrochemical parameters of Cu^+ oxidation by tuning alkyl chain length, polyaromatic structure, and substitute group site of NS4, N, N-bis(2-2((ethylthio)ethyl)-2-naphthamide (NS4-C1) was finally optimized to detect Cu^+ ions owing to the most negative potential and the largest current density. Meanwhile, 9, 10-anthraquinone was designed as a selective pH recognition, while 2, 2'-azino-bis(3-ethylbenzthiazoline-6-sulfonic acid was employed as an inner reference. This single biosensor with both current and potential signal outputs can simultaneously determine Cu^+ concentrations from 0.5 to 9.5 μM, as well as pH values ranging from 6.0 to 8.0. Eventually, the efficient biosensor was contributed to simultaneous detection of Cu^+ and pH in the live brain. The average levels of Cu^+ were first reported in cortex, hippocampus, and striatum in mouse model of Alzheimer disease.

As one of the most common neurodegenerative disorders, Alzheimer's disease (AD) has become a severe social problem with aging of the world population.[1] Copper (Cu) overload coupled with copper-mediated oxidative stress is considered as one of the vital aspects in AD.[2] Most endogenous antioxidants are able to reduce Cu^{2+} to Cu^+. Then, the substochiometric amounts of Cu^+ can trigger the reduction of molecular oxygen to superoxide or hydrogen peroxide.[3] The overproduced reactive oxygen species (ROS) causes the pH decreasing,[4] and further augment oxidative stress.[5] Therefore, development of simultaneously monitoring strategies for Cu^+ and pH in vivo is essential to progress our understanding of the roles that Cu^+ and pH play in pathological and physiological events in the brain.

Electrochemical approaches show remarkable advantages in high temporal resolution and high spatial resolution, as well as real-time measurements in live brains.[6,7] However, in contrast to the pervasive investigation on biosensors for Cu^{2+},[8] fewer work has been reported on development of analytical strategies for Cu^+, although Cu taken up by cells is usually in Cu^+ state.[9] Moreover, even no biosensor has been developed for simultaneous determination of Cu^+ and pH despite of close relationship between Cu^+ and pH in neurodegenerative diseases, because it is still a great challenge to design the selective recognition molecules for Cu^+, as well as to avoid the cross-talk in simultaneous determination.

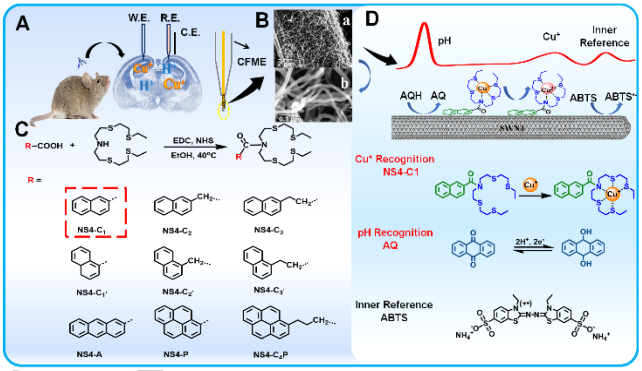

Scheme 1. (A) The developed ratiometric single biosensor for simultaneous evaluating the levels of Cu^+ and pH in a live mouse brain. (B) SEM images of (a) CFME/SWNT and (b) the enlarged image of SWNTs. (C) The general synthesis procedure of NS4s and the corresponding molecular structures. (D) Preparation procedures for the functionalized electrodes.

In this work, we first created a single ratiometric biosensor for simultaneous detection of Cu^+ and pH with significant selectivity and accuracy, and contributed to determination these two speices in the live mouse brains. First of all, a series of novel N, N-bis(2-((2-(ethyl-thio)ethyl)-based derivatives (NS4s) were designed and synthesized for specific recognition of Cu^+ (Scheme 1). The effects of polyaromatic structure, alkyl chain length, and substitute group site on electrochemical parameters of Cu^+ oxidation coordinated with NS4s, including peak potential (E_p), peak current intensity (j_p), surface coverage (Γ), and heterogeneous electron transfer rate (k_s) were systematically investigated. NS4-C_1 was finally selected as an optimized probe to selectively detect Cu^+ in vivo because of the most negative potential to avoid crosstalk of simultaneous detection, as well as the largest current density to enhance sensitivity of biosensor. Meanwhile, 9, 10-anthraquinone (AQ) with oxidation peak (E_p) at -435 mV was optimized as the selective recognition for H^+, while 2, 2'-azino-bis (3-ethylbenzthiazoline-6-sulfonic acid (ABTS) with E_p at ~520 mV was employed as an inner-reference element to improve accuracy. This single biosensor with dual signal outputs can realize the Cu^+ determination with a good linearity in the range of 0.5-9.5 μM, as well as the linear range of 6.0-8.0 for pH determination. Finally, the developed biosensor succeeded in directly evaluating the levels of Cu^+ and pH in a live mouse model of AD. To our knowledge, this is the first report on the accurate concentrations of Cu^+ in a live brain.

As a starting point of this work, a series of NS4 derivatives for specific recognition of Cu^+ were firstly designed and synthesized as demonstrated in Scheme 1C. The molecules compose of three parts: thioether structure with four sulfur atoms linked by

[*] Dr. Wei Liu, Hui Dong, Dr. Limin Zhang, Prof. Yang Tian
Shanghai Key Laboratory of Green Chemistry and Chemical Processes, School of Chemistry and Molecular Engineering, East China Normal University, Dongchuan Road 500, Shanghai 200241 (China)
E-mail: ytian@chem.ecnu.edu.cn; lmzhang@chem.ecnu.edu.cn
† W. Liu. and H. Dong equally contributed to this work.
Supporting information for this article is given via a link at the end of the document.

10.1002/anie.201710863

one imine (NS4) moiety at one end for selectively capturing Cu^+ via coordination interaction, a polyaromatic moiety (naphthalene, nthracene, or pyrene) for anchoring the molecule via hydrophobic and π-π stacking interactions on SWNT surface, and an "arm" of alkyl chain with amide bond linked thioether and polyaromatic foot. All designed molecules were characterized by ^{1}HNMR and HR-MS (Supporting Information (SI), Figure S1-S10). From the typical SEM images, SWNTs were uniformly covered on the carbon fiber microelectrode (CFME) surface (Scheme 1B), and the average length of 2-10 μm was observed with diameter of ~20 nm (Scheme 1Bb). Next, the ligand, NS4-C1 (or other derivatives), was modified on CFME/SWNT surface to form CFME/SWNT/NS4-C1 electrode. The processes for electrode modification were tracked by XPS (SI, Figure S11).

Electrochemical behavior of Cu^+ at CFME/SWNT/NS4-C_1 electrode was then investigated by linear scanning voltammetry (LSV). As shown in Figure 1A, typical LSV curve obtained at CFME/SWNT/NS4-C1 exhibites a well-defined anodic peak with E_p of 0.31 V in aCSF (pH 7.4) in the presence of 10 μM Cu^+, while no faradic peak was observed at CFME/SWNT/NS4-C1 in the absence of Cu^+, indicating this peak is attributed to the oxidation of Cu^+. From XPS data, a new Cu 2p peak located at 932.0 eV was observed after reacted with Cu^+ (SI, Figure S11C). Meanwhile, the S2p 1/2 peak shifts to 163.79 eV due to the formation of S-Cu^+ bond (SI, Figure S11A), but the binding energy of N1s peak decreases by 2.0 eV after reacted with Cu^+ due to the N-Cu feedback coordination (SI, Figure S11B). These results reveal that Cu^+ was stably captured by NS4-C_1 at SWNT surface, in which four S atoms together with one N atom all coordinated with Cu^+. The results from LC-MS (SI, Figure S12) further demonstrated the molar ratio of Cu to NS4 is 1:1.

Next, the effect of arm length on Cu^+ oxidation was investigated using NS4 with different lengths of alkyl chain at two positions of substituent group: Group a: CFME/SWNT/NS4-C_n (C: alkyl chain located at Site 2) and Group b: CFME/SWNT/NS4-C_n' (C': alkyl chain at Site 1). In contrast to CFME/SWNT/NS4-C_1 (0.31 V), E_p positively shifts to 0.34 V and 0.39 V at CFME/SWNT/NS4-C_2, CFME/SWNT/NS4-C_3, respectively (Figure 1), while negligible anodic peak current density (j_p) was obtained at CFME/SWNT/NS4-C_n electrode (SI, Figure S13A). Electrochemical oxidation of Cu^+ at CFME/SWNT electrode modified with NS4s was mainly controlled by two processes: adsorption of Cu^+ via coordination with ligands attached onto CFME/SWNT, and electron transport between Cu^+ and CFME/SWNT. The adsorption ability of Cu^+ at ligands attached onto CFME/SWNT was initially evaluated by the adsorption isotherms. The adsorption amount of Cu^+ was estimated based on Cu^+ oxidation peak current using Equation (1):[10]

$$i_p=(1.62\times10^6)n(1-\alpha)n_a\nu A\Gamma_0^* \quad (1)$$

where i_p, n, α, A, ν, Γ_0^* is oxidation peak current, number of electron transfer, electron transfer coefficient, electrode area, potential sweep rate and surface coverage of species, respectively. The plots of between Γ_0^* of Cu^+ at CFME/SWNT-/NS4-C_1 electrode and Cu^+ concentration (SI, Figure S14) follow the Langmuir Isotherm model described by Equation (2):

$$\Gamma_i=\Gamma_s\beta C_i/(1+\beta C_i) \quad (2)$$

where Γ_i and Γ_s refer to surface adsorption amount at a given concentration and saturated surface coverage, respectively. C_i is concentration of bulk solution, β is equilibrium parameter in an

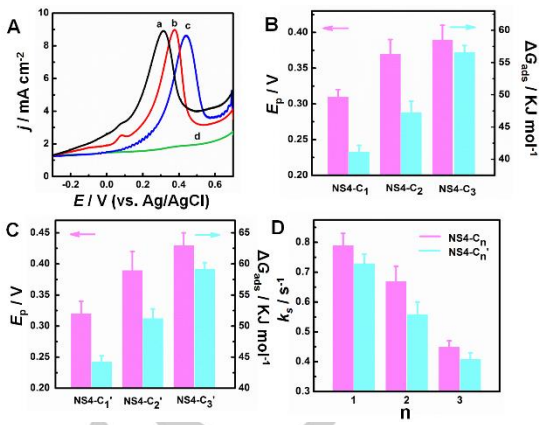

Figure 1. (A) Typical LSV curves obtained at CFME/SWNT/NS4-C_n (a: n=1, b: n=2, c: n=3) electrodes in aCSF solution (pH 7.4) in the presence (a-c) and (d) absence of 10 μM Cu^+. (B-C) E_p of Cu^+ oxidation peaks and corresponding ΔG_{ads} values of ligands obtained at (B) CFME/SWNT/NS4-C_n, and (C) CFME/SWNT/NS4-C_n' electrodes. (D) k_s values of Cu^+ oxidation obtained at CFME/SWNT/NS4-C_n, and CFME/SWNT/NS4-C_n' electrodes.

adsorption isotherm. Corresponding Γ_s and ΔG_{ads} values were calculated according to –RTln(18.9β). As shown in Table S1, negligible variation among Γ_s at CFME/SWNT/NS4-C_n suggests the surface coverage of Cu^+ coordinated with ligands is less affected by chain length, resulting in comparable j_p values. However, ΔG_{ads} increases with increasing length of alkyl chain owing to more hydrophobicity of NS4s with longer chain.[11] Since $\Delta G_{ads} = -nFE_p$, the weakest adsorption energy of NS4-C_1 among NS4-C_n eventually results in the most negative E_p, which is consistent with the results from Figure 1B and 1C.In order to further elucidate the effect of alkyl chain length on the electrochemical parameter, k_s of Cu^+ coordinated with NS4 complex was determined by Laviron method.[12] k_s were calculated to be 0.79±0.04 s^{-1} for NS4-C_1, 0.67±0.05 s^{-1} for NS4- C_2, and 0.40±0.02 s^{-1} for NS4-C_3 (SI, Table S1). The results indicate that the longer distance between Cu^+ center and CFME/SWNT with longer alkyl chain would decrease electron transfer rate of Cu^+. Similar electrochemical results were also observed for NS4 derivatives in Group b (NS4-C_n') (Figure 1C). Interestingly, no obvious difference was observed for using NS4 derivatives with two distinct sites of substituent group: a and b (SI, Figure S15).

Then, the effect of polyaromatic moiety was studied. E_p positively shifts with increasing size of polyaromatic footprint, which increased by 40 mV for NS4-A, and 70 mV for NS4-P than that for NS4-C_1 (Figure 2A). ΔG_{ads} values of three derivatives also went up to -50.59 KJ mol^{-1} for NS4-A, and further to -62.43 KJ mol^{-1} for NS4-P (Figure 2B). The smallest delocalized π system of naphthalene leads to the weakest π-π interaction among three ligands. The averaged ΔG_{ads} of 15-20 KJ mol^{-1} between polyaromatic molecule with each increase of aromatic ring and CNTs substrate is consistent with previous reports.[13] Accordingly, E_p positively shifts with increasing polyaromatic foot (Figure 2B). On the other hand, j_p value greatly decreased by 26% at CFME/SWNT/NS4-A, and by 41% for CFME/SWNT/NS4-P compared with that at CFME/SWNT/NS4-C_1 (Figure 2C) due to decreasing Γ_s value of Cu^+ at corresponding surfaces. These results demonstrate that the smallest polyaromatic structure of naphthalene moiety is most beneficial for oxidation of Cu^+

10.1002/anie.201710863

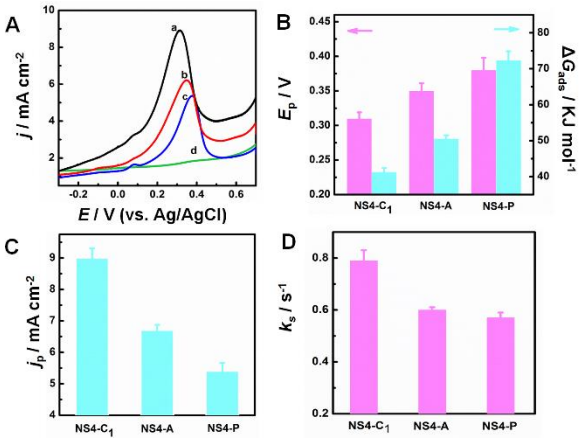

Figure 2. (A) Typical LSV curves obtained at (a) CFME/SWNT/NS4-C_1, (b) CFME/SWNT/NS4-A, and (c) CFME/SWNT/NS4-P in aCSF solution (pH 7.4) in the presence (a-c) and (d) in the absence of 10 μM Cu^+, respectively. (B) E_p of Cu^+ oxidation peaks and corresponding ΔG_{ads} values of ligands obtained at CFME/SWNT modified by NS4-C_1, NS4-A, and NS4-P. (C) j_p and (D) k_s values of Cu^+ oxidation peaks obtained at CFME/SWNT/NS4-C_1, CFME/SWNT/NS4-A, and CFME/SWNT/NS4-P electrodes.

coordinated with NS4-C_1 at CFME/SWNT, leading to the most negative E_p and the highest j_p value.

For confirming the results demonstrated above, NS4-C_4P with the longest chain and the largest footprint was synthesized. As expected, the most positive E_p (0.46 V) and the smallest j_p was obtained at (SI, Figure S16) at CFME/SWNT/NS4-C_4P, further demonstrating that the electrochemical behavior can be rationally tuned through optimizing polyaromatic structure and alkyl chain length. Accordingly, NS4-C_1 molecule was selected as a promising candidate for in vivo monitoring of Cu^+ levels because of the most negative potential to avoid potential-crosstalk of simultaneous detection, as well as the largest current density to enhance sensitivity of biosensor.

Then, AQ, NS4-C1, and ABTS, were simultaneously immobilized at CFME/SWNTs via hydrophobic and π-π stacking interactions. Two types of S 2p peaks (S=O and S-C) located at ~164.3 eV and ~169.5 eV at SWNT/AQ+NS4-C_1+ABTS were obtained in XPS results (SI, Figure S17A). Meanwhile, the corresponding N1s spectra can be deconvoluted into three peaks: ~399 eV ascribed to N=C, ~400 eV to N-C, and ~403 eV to N=N (SI, Figure S17B), confirming the successful immobilization of NS4-C_1 and ABTS onto the SWNTs. The modification of AQ on the SWNTs was characterized by FTIR spectra (SI, Figure S18). Each modification step was next characterized by LSV (SI, Figure S19). No response was observed at CFME/SWNT in aCSF (pH 7.4), while oxidation peaks at -435 mV and 520 mV were clearly observed at CFME/SWNT/AQ and CFME/SWNT/ABTS, respectively, attributed to the oxidation of AQ and ABTS attached on CFME/SWNT electrode (Figure 3A). After AQ, NS4-C_1, and ABTS were co-immobilized on the CFME/SWNT, two anodic peaks were observed at -435 mV and 520 mV for CFME/SWNT/-AQ+NS4-C_1+ABTS. This electrode exhibited good stability after consecutive scanning for 500 cycles (SI, Figure S20), which thanks to hydrophobic and π-π stacking interactions between molecules and SWNTs. A new anodic peak appeared at ~300 mV with the addition of Cu^+ into aCSF (pH 7.4). Such anodic peak

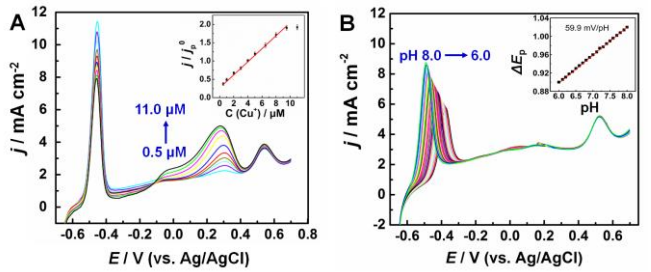

Figure 3. (A) LSVs obtained at CFME/SWNT/AQ+NS4-C_1+ ABTS electrode in aCSF (pH 7.4) containing different concentrations of Cu^+ from 0.5 to 11.0 μM, respectively. Inset: calibration plot of j_p/j_p^0 with different Cu^+ concentrations. (B) LSVs obtained at CFME/SWNT/AQ+NS4-C_1+ABTS electrode in aCSF solution with different pH values ranging from 6.0 to 8.0. Inset: Calibration plot of ΔE_p against different pH.

disappeared with a slight negative shift (~5 mV) of AQ peak potential after EDTA was added (Figure 3B), because EDTA is only soluble in alkaline solution and pH of EDTA solution was adjusted to ~9.0. This result indicates that this anodic peak is ascribed to the oxidation of Cu^+ captured by NS4-C1 confined on the electrode surface, because EDTA took Cu^+ away from NS4-C1-Cu^+ complex. Moreover, j_p observed at ~300 mV gradually increased with increasing concentrations of Cu^+, while that of ABTS at ~520 mV (j_p^0) kept almost constant (Figure 3A), resulting in the ratiometric determination of Cu^+ with high accuracy. Moreover, j_p/j_p^0 exhibites a good linearity with the concentration of Cu^+ in the range of 0.5 to 9.5 μM with a detection limit down to ~500 nM (S/N = 3:1). The electrochemical signals for AQ and ABTS at CFME/SWNT/AQ+NS4-C_1+ABTS were estimated to be ~9.0-fold greater than that obtained at CFME/AQ+NS4-C_1+ABTS, owing to the large surface area and electrocatalytic activity of SWNTs (SI, Figure S21). Moreove, NS4-C_1 exhibited fast response time for Cu^+ within 1 min (SI, Figure S22).

On the other hand, the pH dependence of CFME/SWNT/AQ +NS4-C_1+ABTS electrode was studied (Figure 3B). The anodic peak potential for AQ (E_p(AQ)) positively shifted with pH changed from 8.0 to 6.0, while the anodic peak potential of ABTS E_p(ABTS) stayed constant. The separation between E_p(ABTS) and E_p(AQ) ($\Delta E_p = E_p$(ABTS)- E_p(AQ)) exhibits a good linearity from pH 6.0 to 8.0 with a detection limit of 0.05 pH with a gradient of 60 mV/pH which well accord with the theoretically value from Nernst equation (inset in Figure 3B). More importantly, there is negligible cross-talk between pH and Cu^+ determination. The maximum of current fluctuation is no more than 5% when pH ranges from 6.0 to 8.0. Meanwhile, ΔE_p is almost unchanged (< 2 mV) with Cu^+ concentration varing from 1 μM to 10 μM (SI, Figure S23).

Selectivity is also a great challenge for in vivo analysis in the complicated brain system. The selectivity and competition test of the develop biosensor for simultaneous determination of Cu^+ and pH was examined against metal ions, amino acid, and other potential interferences. No obvious current (< 4.0%) was observed for anodic peak of Cu^+ upon the addition of these interferences and even Cu-containing proteins (SI, Figure S24). Meanwhile, no obvious change of ΔE_p value (<1.0%) upon the addition of various interferences. All the results indicate high selectivity of the present biosensor for simultaneous detection of of Cu^+ and pH.

10.1002/anie.201710863

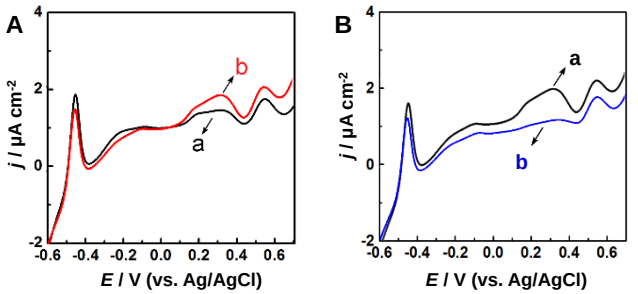

Figure 4. (A) LSVs obtained at CFME/SWNT/AQ+NS4-C_1 +ABTS electrode in (a) normal mouse brain and (b) mouse brain with AD. (B) LSVs of CFME/SWNT/AQ+NS4-C_1+ABTS electrode in (a) mouse brain with AD, and (b) followed by microinjection of 0.1 mM EDTA (pH 9.0). Scan rate: 20 mV s^{-1}.

The developed ratiometric biosensor for simultaneous quantification of Cu^+ and pH with remarkable analytical performance, along with unique properties of CFME including easy to insert in the brain and good biocompati-bility, provided a reliable in vivo platform for assaying pH and Cu^+ levels in the live mouse brain. Three anodic peaks were clearly observed at -425 mV, 310 mV and 530 mV at CFME/SWNT/AQ+NS4-C_1+ABTS electrode in the mouse brain (Curve a, Figure 4A), which are ascribed to the oxidation peak of AQ, Cu^+, and ABTS. According to the post-calibration (SI, Figure S25), the basal levels of pH were estimated to be 7.25 ± 0.03, 7.15±0.07, and 7.15 ± 0.07 in striatum, hippocampus, and cortex, which were similar as those previously reported.[14] Unexpectedly, negligible pH variations were observed in these regions of mouse model of AD (Figure 4A). Meanwhile, the measurements demonstrate that basal levels of Cu^+ in the normal mouse brain: 2.35 ± 0.22 μM in striatum, 2.08 ± 0.20 in hippocampus, and 1.75 ± 0.13 in cortex. However, the levels of Cu^+ increased to 4.43 ± 0.40 in striatum, 4.11 ± 0.26 in hippocampus, and 2.65 ± 0.31 in cortex in mouse model of AD (SI, Table S2). To the best of our knowledge, this is the first report for the accurate concentrations of Cu^+ in the normal mouse brain and mouse model of AD. The increased Cu^+ concentration observed in mouse model of AD might be generated from the reduction of Cu^{2+} by overexpressed amyloid precursor protein (APP).[15] APP is involved in Cu homeostasis, and possesses a copper binding site in its NH_2-terminal cysteine-rich domain,[15a] which can reduce Cu^{2+} to Cu^+. To further identify the origination of oxidation current at ~310 mV, 0.1 mM EDTA solution (pH 9.0) was exogenously microinjected into the vicinity of the implanted electrode. This peak rapidly decreased to base line, confirming that the anodic peak was caused by oxidation of Cu^+ (Figure 4B). Meanwhile, E_p(AQ) had 5 mV negative shift when basic EDTA was microinjected into the striatum, while the peak of ABTS stayed constant. This phenomenon is similar to that of in vitro experiment. As a control, the infusion of aCSF (pH 7.4) could not give rise to any apparent shifting of pH. In addition, the standard deviation of j_p/j_p^0 of five developed biosensors tested in striatum of the same mouse brain did not exceed 4.0% for Cu^+, 1.0% for pH, indicating good reproducibility of the present biosensor (SI, Figure S26).

In summary, we havedesigned and synthesized a series of NS4 derivatives for specific recognition of Cu^+. Through rationally tuning lengths of alkyl chain and polyaromatic structures of designing organic molecules, NS4-C1 was optimized for Cu^+ specific recognition. The principles have provided very useful information for efficient construction of molecule-based biosensor with high selectivity. Combination with AQ and ABTS employed for pH indicator and inner-reference element, a single ratiometric biosensor has been developed for simultaneous determination of Cu^+ and pH with highly efficient performance based on both current and potential signal outputs. The unique analytical performance has eventually opened up a new way to evaluate the levels of Cu^+ and pH in rat brain with AD in vivo. The research has first reported the higher concentration of Cu^+ in mouse model of AD, which may give insight understanding to the damage of AD on brain function. More importantly, the present study has also provided a methodology for designing the single biosensors for determination of multi-species, which may be closely related to physiological and pathological events of brain.

Acknowledgements. Support from NSFC for Distinguished Young Scholars (21325521) and NSFC (21635003 for Y. T., 21305104 and 21675054 for L. Z.) is gratefully acknowledged.

Keyword: Brain chemistry • Biosensors • Analytical Methods • Cuprous ion • pH

[1] a) R. E. Tanzi, L. Bertram. *Cell,* **2005,** *120,* 545; b) P. Shrestha, E. Klann. *Nature* **2016,** *531,* 450; c) S. C. P. Williams, *Nature* **2013,** *502,* S84.
[2] A. I. Bush,*Trends Neurosci.* **2003,** *26,* 207.
[3] Cooper, G. J. S. *Drugs* **2011,** *71,* 1281
[4] a) X. Ma, Y. Wang, T. Zhao, T. Li, L. Su, Z. Wang, G. Huang, B. Summer, J. Gao, *J. Am. Chem. Soc.* **2014,** *136,* 11085; b) B. A. Webb, M. Chimenti, M. P. Jacobson, D. L. Barber, *Nat. Rev. Cancer* **2011**, *11*, 671.
[5] a) C. S. Atwood, R. D. Moir, X. D. Huang, R. C. Scarpa, N. Bacarra, D. M. Romano, M. K. Hartshorn, R. E. Tanzi, A. I. Bush, *J. Biol. Chem.* **1998,** *273,* 12817; b) A. D. Milito, R. Canese, M. L. Marino, M. Borghi, M. Lero, A. Villa, G. Venturi, F. Lozupone, E. Lessi, M. Logozzi, P. D. Mina, M. Santinami, M. Rodolfo, F. Podo, L. Rivoltini, S. Fais, S. *Int. J. Cancer* **2010**, *127*, 207.
[6] a) L. Zhang, Y. Han, F. Zhao, G. Shi, Y. Tian, *Anal. Chem.* **2015,** *87,* 2931; b) L, Shuai, A. Zhu, T. Zhou, J. Z. H. Zhang, Y. Tian, *Anal. Chem.* **2017,** *89,* 6656; c) M. Jung, G. Shi, L. Borland, A. C. Michael, S. G. Weber, *Anal. Chem.* **2006**, 78, 1755.
[7] a) D. Kato, K. Goto, S. Fujii, A. Takatsu, S. Hirono, O. Niwa, *Anal. Chem.* **2011**, 83, 7595; b) M. A. Makos, D. M. Omiatek, A. G. Ewing, M. L. Heien, *Langmuir* **2010,** *26,* 10386; c) N. J. Finnerty, F. B. Bolger, E. Palsson, J. P. Lowry, *ACS Chem. Neurosci.* **2013,** *4,* 825. d) Y. Liu, Z. Jin, Y. Liu, Y, Qin, J. Xu, C. Fan, W. Huang, *Angew. Chem. Int. Ed.* **2016**, *128,* 4613.
[8] a) X. Chai, X. Zhou, Y. Qin, L. Zhang, G. Shi, Y. Tian, *Angew. Chem. Int. Ed.* **2013,** *52,* 8129 b) Y. Luo, L. Zhang, W. Liu, Y. Yu, Y. Tian, *Angew. Chem. Int. Ed.* **2015,** *54,* 14053; c) A. Zhu, Q. Qu, X. Shao, B. Kong, Y. Tian, *Angew. Chem. Int. Ed.* **2012,** *51,* 7185; d) W. Qu, Y. Liu, D. Liu, Z. Wang, X. Jiang. *Angew. Chem. Int. Ed.* **2011,** *50,* 3442.
[9] L. Zeng, E. W. Miller, A. Pralle, E. Y. Isacoff, C. J. Chang, *J. Am. Chem. Soc.* **2006,** *128,* 10.
[10] E. Laviron, *Electroanal. Chem. Interfacial Electrochem.* **1974,** *52,* 355.
[11] R. Smith, C. Tanford, C. *Proc. Natl. Acad. Sci. U S A.* **1973,** *70,* 289.
[12] E. Laviron, *J. Electroanal. Chem.* **1979,** *101,* 19.
13] M. Lu, R. G. Compton, *Analyst* **2014**, *139*, 2397.
[14] a) J. Zhou, L. Zhang, Y. Tian, *Anal. Chem.* **2016,** *88,* 2113; b) F. Zhao, L. Zhang, A. Zhu, G. Shi, Y. Tian, *Chem. Commun.* **2016,** *52,* 3717; c) K. Kogure, O. F. Alonso, E. Martinez, *Brain. Res.* **1980**, *195*, 95.
[15] a) G. Multhaup, A. Schlicksupp, L. Hesse, D. Beher, T. Ruppert, C. L. Masters, K. Beyreuther, *Science*, **1996**, *271*, 1406; b) H. Basun, L. G. Forssell, L. Wetterberg, B. Winblad, *J. Neural. Transm, Park. Dis. Dement. Sect.* **1991,** *3,* 231.

10.1002/anie.201710863

WILEY-VCH

COMMUNICATION

Cuprous (Cu^+) and pH play vital roles in the physiological and pathological events of brain. In this work, a series of NS4s molecules were designed and synthesized for specific recognition of Cu^+. On the basis of the optimized results, an efficient biosensor was created for ratiometric monitoring of Cu^+ and pH in a mouse model of AD, using two types of electrical signal outputs. The average levels of Cu^+ were firstly reported in the cortex, hippocampus, and striatum in mouse model of AD.

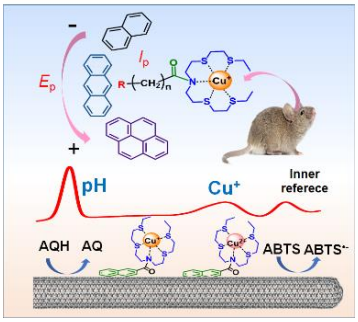

Wei Liu,[†] Hui Dong,[†] Limin Zhang,* Yang Tian*

Page 1. – Page 4.

Developing an Efficient Biosensor for In Vivo Quantification of Cu^+ and pH in the Brain Based on Rational Design and Synthesis of Recognition Molecules